Heliyon 10 (2024) e30336

Contents lists available at ScienceDirect

Heliyon

journal homepage: www.cell.com/heliyon

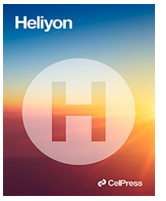

Research article

Uncovering the shared neuro-immune-related regulatory mechanisms between spinal cord injury and osteoarthritis

Yuxin Zhang [a,b,c,1], Dahe Zhang [b,1], Xin Jiao [c], Xiaokun Yue [c], Bin Cai [a], Shenji Lu [a], Renjie Xu [d,*]

[a] *Department of Rehabilitation Medicine, Fengcheng branch, Shanghai Ninth People's Hospital, Shanghai Jiao Tong University School of Medicine, Shanghai, 200011, China*

[b] *Department of Oral Surgery, Shanghai Ninth People's Hospital, Shanghai Jiao Tong University School of Medicine, College of Stomatology, Shanghai Jiao Tong University, National Center for Stomatology, National Clinical Research Center for Oral Diseases, Shanghai Key Laboratory of Stomatology, Shanghai, 200011, China*

[c] *Shanghai Key Laboratory of Orthopedic Implants, Shanghai Ninth People's Hospital, Shanghai Jiao Tong University School of Medicine, Shanghai, 200011, China*

[d] *Department of Rehabilitation Medicine, Kunshan Rehabilitation Hospital, Suzhou 210000, Jiangsu, China*

A R T I C L E I N F O

Keywords:
Spinal cord injury
Osteoarthritis
WGCNA
Immuno-inflammation
PPI network
miRNA

A B S T R A C T

Adults with spinal cord injury (SCI), a destructive neurological injury, have a significantly higher incidence of osteoarthritis (OA), a highly prevalent chronic joint disorder. This study aimed to dissect the neuroimmune-related regulatory mechanisms of SCI and OA using bioinformatics analysis. Using microarray data from the Gene Expression Omnibus database, differentially expressed genes (DEGs) were screened between SCI and sham samples and between OA and control samples. Common DEGs were used to construct a protein-protein interaction (PPI) network. Weighted gene co-expression network analysis (WGCNA) was used to mine SCI- and OA-related modules. Shared miRNAs were identified, and target genes were predicted using the Human MicroRNA Disease Database (HMDD) database. A miRNA-gene-pathway regulatory network was constructed with overlapping genes, miRNAs, and significantly enriched pathways. Finally, the expression of the identified genes and miRNAs was verified using RT-qPCR. In both the SCI and OA groups, 185 common DEGs were identified, and three hub clusters were obtained from the PPI network. WGCNA revealed three SCI-related modules and two OA-related modules. There were 43 overlapping genes between the PPI network clusters and the WGCNA network modules. Seventeen miRNAs shared between patients with SCI and OA were identified. A regulatory network consisting of five genes, six miRNAs, and six signaling pathways was constructed. Upregulation of *CD44*, *TGFBR1*, *CCR5*, and *IGF1*, while lower levels of miR-125b-5p, miR-130a-3p, miR-16-5p, miR-204-5p, and miR-204-3p in both SCI and OA were successfully verified using RT-qPCR. Our study suggests that a miRNA-gene-pathway network is implicated in the neuroimmune-related regulatory mechanisms of SCI and OA. *CD44*, *TGFBR1*, *CCR5*, and *IGF1*, and their related miRNAs (miR-125b-5p, miR-130a-3p, miR-16-5p, miR-204-5p, and miR-204-3p) may serve as promising biomarkers and candidate therapeutic targets for SCI and OA.

* Corresponding author. Kunshan Rehabilitation Hospital, No.888 Yingbin East Road, Zhoushi, Kunshan, Suzhou, Jiangsu, 210000, China.
E-mail address: keyanqiufazhan@163.com (R. Xu).

[1] Co-first authors.

https://doi.org/10.1016/j.heliyon.2024.e30336
Received 10 May 2023; Received in revised form 21 April 2024; Accepted 24 April 2024
Available online 25 April 2024

1. Introduction

Spinal cord injury (SCI) is a devastating and intractable neurological disease that leads to physiological dysfunction below the damaged segments [1]. SCI has increased global incidence in recent years and remains a significant source of enormous economic burden on society [2]. Osteoarthritis (OA) is a highly prevalent musculoskeletal disease that damages the joint cartilage and affects other joint tissues [3]. It negatively affects people's daily lives and is responsible for significant socioeconomic costs [4]. There is evidence that the incidence and risk of OA are significantly elevated in adults with SCI [5]. SCI leads to bone loss, low bone mineral density, and muscle atrophy [6,7]. Metabolic dysfunction induced by SCI exacerbates bone loss, thereby increasing the risk of bone fractures and promoting abnormal ossification [8]. Additionally, joint contractures are aggravated by motor dysfunction and decreased plasticity after SCI [9]. All of these musculoskeletal disorders contribute to the high risk and incidence of OA in the population with SCI.

Neuroinflammation plays a key role in the pathophysiology of SCI, involving activation of various inflammatory cell types, such as macrophages, neutrophils, and lymphocytes, and release of inflammatory cytokines, such as tumor necrosis factor (TNF)-α and interleukin (IL)-6 [10]. Inflammation is also a well-established cause of OA, resulting in an imbalance between anabolic and katabolic processes [11,12]. Moreover, a recent study provided evidence that communication between circulating immune cells (e.g., macrophages, T cells, and neutrophils) and neurons is critical for pain-related diseases such as SCI and OA [13]. It has been reported that the expression of pro-inflammatory cytokines (IL-1β and IL-6) could be upregulated in SCI or OA, while the levels of anti-inflammatory cytokines (IL-10 and tumor growth factor-β) were decreased [14,15]. These inflammation- and immune-related mechanisms may explain the high susceptibility of SCI to OA. Deciphering the underlying mechanisms can help explore novel therapeutic possibilities for patients with concurrent SCI and OA.

Weighted gene co-expression network analysis (WGCNA) is a widely used method for constructing functional networks to investigate the correlation between gene expression and clinical data at an unbiased system level [16]. It allows the simultaneous identification of many hub genes and provides a solution for the complicated pathogenesis of diseases [17]. WGCNA identified common hub genes and signaling pathways between Alzheimer's disease and type 2 diabetes mellitus [18] and between systemic lupus erythematosus and pulmonary arterial hypertension [19]. Li et al. [20] identified eight immune-related core genes (*FZD7*, *IRAK3*, *KDELR3*, *PHC2*, *RHOB*, *RNF170*, *SOX13*, and *ZKSCAN4*) that could be used to diagnose patients with OA and metabolic syndrome. Another study identified *B2m*, *Itgb5*, and *Vav1* as immune-related hub genes in SCI and found that *B2m* and *Itgb5* were located in microglia, whereas *Vav1* was mainly expressed in macrophages [21]. Furthermore, molecular docking showed that the proteins corresponding to *B2m*, *Itgb5*, and *Vav1* could accurately bind to decitabine, as well as pro-inflammatory factor (TNF-α and IL-1β) levels were decreased, and anti-inflammatory factor (IL-4, and IL-10) levels were increased in decitabine-treated SCI mice. However, the neuroimmune-related regulatory mechanisms underlying SCI and OA remain unclear.

SCI is divided into acute, middle, and late stages. Studies have shown that after SCI, most of the dynamic changes occur three days after injury; by day 14, a second wave of microglia activation appears, accompanied by changes in various cell types, including neurons; by day 38, the dominant cell types still deviate greatly from the undamaged state, showing long-term changes [18,19]. OA is a chronic degenerative disease that can be divided into four stages: pre-stage, early stage, advanced stage, and late stage. Many reports have shown that after two weeks of injury, the OA rat model is in the early stages of OA [20–22]. In this study, to eliminate analytical biases caused by different time points, we chose a specific time point of two weeks for analysis. Combining transcriptome and clinical data, we identified common differentially expressed genes (DEGs) in SCI and OA and built a protein-protein interaction (PPI) network. Using the WGCNA network, we mined SCI-related- and OA-related modules and then identified the shared signature genes. The miRNAs shared between SCI and OA were extracted and used to construct a miRNA-gene pathway network, and the identified DEGs were used to establish a transcriptional factor regulatory network. The identified genes were used for the immune analysis. Finally, the expression of the identified key signature genes was validated using independent datasets and tissue samples.

2. Materials and methods

2.1. Data download and preprocessing

From the National Center for Biotechnology Information Gene Expression Omnibus (GEO) database (http://www.ncbi.nlm.nih.gov/geo/), we downloaded the GSE45006 [22] and GSE20907 [23] datasets of SCI (GPL1355[Rat230_2] Affymetrix Rat Genome 230 2.0 Array platform). In GSE45006, we selected four spinal cord samples harvested from rats two weeks after SCI and four sham samples as the discovery cohort. In GSE20907, we selected two spinal cord samples from rats with two weeks of SCI and four sham samples as the validation cohort.

For OA, we obtained GSE103416 [24] (GPL17117[RaGene-2_0-st] Affymetrix Rat Gene 2.0 ST Array [transcript (gene) version]) and GSE42295 (GPL1355[Rat230_2] Affymetrix Rat Genome 230 2.0 Array). We focused on the OA samples harvested at two weeks in accordance with the SCI samples. Therefore, we selected four OA tissue samples and four control samples from GSE103416 and three OA tissue samples and three control samples from GSE42295. These were used as discovery and validation cohorts for OA, respectively.

2.2. Screening significant DEGs in SCI and OA

Using limma [25] package in R software (version3.34.7, https://bioconductor. org/packages/release/bioc/html/limma.html), with a false discovery rate (FDR) < 0.05 and $|\text{Log}_2$ fold change (FC)$| > 1$ as the cutoff, we screened DEGs between SCI and sham samples, and between OA and control samples. Hierarchical clustering analysis was performed for all identified DEGs using the pheatmap package [26] (version 1.0.8) in R. The common DEGs shared by SCI and OA were subjected to subsequent gene ontology (GO) [27] function and Kyoto Encyclopedia of Genes and Genomes (KEGG) [28] pathway enrichment analysis (FDR <0.05) using the Database for Annotation, Visualization, and Integrated Discovery software (version 6.8).

2.3. PPI network analysis

To investigate the interactions between shared DEGs in SCI and OA, we constructed a PPI network using STRING [29] (version 11.0). The confidence score cutoff was set at 0.4. The topological properties of the network were analyzed using the CentiScaPe plugin [30] (version 2.2) of the Cytoscape [31] software (version 3.9.0), including the average shortest path length, betweenness centrality (a parameter of network strength), closeness centrality (closeness of a node to other nodes), and degree (the number of interactions with a specific node). Nodes with the highest degrees were defined as hub genes. Network modules (degree cutoff $= 2$, node score cutoff $=$ 0.2, and K-core $= 2$) were mined using the Mcode plugin (version 1.4.2). The significant GO biological processes of these modules ($p <$ 0.05) were determined using the BINGO plugin (version 2.44). Genes in the identified network modules were defined using gene set 1.

2.4. WGCNA network analysis

Using the WGCNA package (version 1.61) in R, WGCNA [32] was applied to explore the gene co-expression modules related to SCI and OA in the GSE45006 and GSE103416 datasets, respectively. Specifically, appropriate soft power β of the adjacency matrix was determined according to scale-free network property. The soft power β was set to 12 and 10 for GSE45006 and GSE103416, respectively. The topological overlap matrix (TOM) and the corresponding dissimilarity (1-TOM) were then calculated. A hierarchical clustering dendrogram was further constructed, and genes with similar expression were clustered into modules with the cutoff of module size $\geq$100 and cutHeight $= 0.995$.

The selected SCI-related- and OA-related modules then overlapped. The intersection of the overlapping module genes (gene set 2) and shared DEGs was defined as gene set 3 and used in subsequent analyses.

2.5. The miRNA-target gene network analysis

Human MicroRNA Disease Database (HMDD, version 3.2; http://www.cuilab. cn/hmdd) contained many miRNA-disease association entries [33]. We downloaded SCI-related- and OA-related miRNAs from the HMDD database and identified the common miRNAs shared by both diseases. Target genes of common miRNAs were predicted using the miRWalk database [34] (version 3.0). Subsequently, the genes shared between the predicted target genes and gene set 3 were selected and combined with the shared miRNAs to construct an miRNA-target gene network.

KEGG pathway enrichment analysis was performed for the genes in the miRNA-target gene network to identify significantly enriched signaling pathways ($p < 0.05$). The mirPathv3 database is dedicated to deciphering the regulatory roles of miRNAs and rendering KEGG pathway annotations of miRNAs [35]. We identified significant KEGG signaling pathways regulated by these miRNAs contained in the miRNA-target gene network. Finally, overlapping signaling pathways for genes and miRNAs in the network were selected to construct regulatory networks.

2.6. Analysis of the transcriptional factors (TFs) regulatory network and correlation between genes and immune cells

The database of Transcriptional Regulatory Relationships Unraveled by Sentence-based Text mining (https://www.grnpedia.org/trrust/) was used to download all TFs and the connection information of the regulated target genes, which were retained to construct a regulatory network.

In addition, the Tumor Immune Estimation Resource (https://cistrome.shinyapps.io/timer/) was used to evaluate the proportion of immune cells based on the GSE45006 and GSE103416 datasets, and the Kruskal-Wallis test was employed to compare the distribution differences in the proportion of each immune cell. Next, the correlation between the significantly different distributions of immune cells and the expression levels of the five important genes was analyzed.

2.7. Expression validation of common key genes in validation sets

We analyzed the expression levels of common key genes in SCI and sham samples from the GSE45006 and GSE20907 datasets, respectively. The expression levels of key genes in the OA and control samples were compared using the GSE103416 and GSE42295 datasets, respectively. Comparisons between groups were performed using Student's t-test.

2.8. Real-time quantitative PCR (RT-qPCR)

The expression levels of the five identified DEGs (*CD44*, *TGFBR1*, *CCR5*, *CLEC7A*, and *IGF1*) were significantly associated with SCI and OA, and the levels of their related miRNAs (miR-125b-5p, miR-130a-3p, miR-16-5p, miR-204-5p, miR-204-3p, and hsa-miR-30b-3p) were verified in tissue samples using RT-qPCR. The SCI rat model was constructed as previously reported [36,37], and the OA rat model was established based on our previous research [38]. Rat thoracic spinal cord samples from the control and SCI groups (n = 5 per group) and rat knee joint synovium samples from the control and OA groups (n = 5 per group) were collected. Total RNA was extracted from all the samples using the RNAiso Plus kit (Trizol, Takara, Beijing, China) according to the instructions of the manufacturer and then was reverse transcribed into cDNA using the PrimeScript™ II 1st Strand cDNA synthesis kit (Takara). The RT-qPCR reaction was initiated at 95 °C for 3 min, followed by 40 cycles of 95 °C for 10 s and 60 °C for 30 s. The sequences of all primers are listed in Table 1. The levels of all the miRNAs were measured using the stem-loop method, with U6 serving as the reference gene. *GAPDH* was used as a housekeeping gene to calculate the DEGs. The levels of related DEGs and miRNAs were all analyzed using the $2-\Delta\Delta Ct$ method. All animal experiments were conducted in accordance with the National Medical Advisory Committee guidelines and approved by the Animal Care and Use Committee of Shanghai Ninth People's Hospital, Shanghai Jiao Tong University School of Medicine.

3. Results

3.1. A total of 185 common DEGs identified in SCI and OA

The overall analytical flowchart of the study is shown in Fig. 1. We paired GSE45006 and GSE103416 as the discovery cohorts for SCI and OA, respectively. In GSE45006, 1475 DEGs (FDR < 0.05, $|Log_2FC| > 1$) were identified in SCI samples compared with sham samples, including 557 downregulated and 918 upregulated DEGs (Fig. 2A). Using the GSE103416 data, 1164 DEGs (FDR < 0.05, $|Log_2FC| > 1$) were identified in OA samples relative to control samples, consisting of 557 downregulated and 918 upregulated DEGs (Fig. 2B).

As shown in the Venn diagram (Fig. 2C), SCI and OA shared 185 common DEGs, including 52 downregulated and 133 upregulated DEGs. These common DEGs were significantly enriched in 31 GO biological processes and 16 KEGG signaling pathways. The GO

Table 1
The sequences of all primers.

Primer	Sequences (5'-3')
rat-U6	RT: CGCTTCACGAATTTGCGTGTCAT
	F: GCTTCGGCAGCACATATACTAAAAT
	R: CGCTTCACGAATTTGCGTGTCAT
rno-miR-125b-5p	RT: GTCGTATCCAGTGCAGGGTCCGAGGTATTCGCACT GGATACGACTCACAA
	F: TCCCTGAGACCCTAAC
rno-miR-130a-3p	RT: GTCGTATCCAGTGCAGGGTCCGAGGTATTCGCACT GGATACGACATGCCC
	F: GCGCCAGTGCAATGTTAAAA
rno-miR-16-5p	RT: GTCGTATCCAGTGCAGGGTCCGAGGTATTCGCACT GGATACGACCGCCAA
	F: GCGCTAGCAGCACGTAAATA
rno-miR-204-5p	RT: GTCGTATCCAGTGCAGGGTCCGAGGTATTCGCACT GGATACGACAGGCAT
	F: GCCGTTCCCTTTGTCATCCT
rno-miR-204-3p	RT: GTCGTATCCAGTGCAGGGTCCGAGGTATTCGCACT GGATACGACAACGTC
	F: ATGCTGGGAAGGCAAAGG
rno-miR-30b-3p	RT: GTCGTATCCAGTGCAGGGTCCGAGGTATTCGCACT GGATACGACGACGTA
	F: GCCCTGGGATGTGGATGTT
Universal downstream primer	GTGCAGGGTCCGAGGT
GAPDH	F: AGACAGCCGCATCTTCTTGT
	R: CTTGCCGTGGGTAGAGTCAT
CD44	F: GATGCAAGAAGAGGTGGAAGTC
	R: CGTTGGAGTCAGTAGCAAGAGTC
TGFBR1	F: GTCTCTGCTTTGTCTCAGTCACC
	R: AAGGTCCTGTAGTTGGGAGTTC
CCR5	F: ACCCCTACTTGTCATGGTCATC
	R: GTCATCCCAAGAGTCTCTGTCAC
CLEC7A	F: GTGCTTGCTCACAGTAGTGGTC
	R: TAGTTCTGCCCTTGCCTGTAGT
IGF1	F: CACATCTCTTCTACCTGGCACTC
	R: GTACATCTCCAGCCTCCTCAGAT

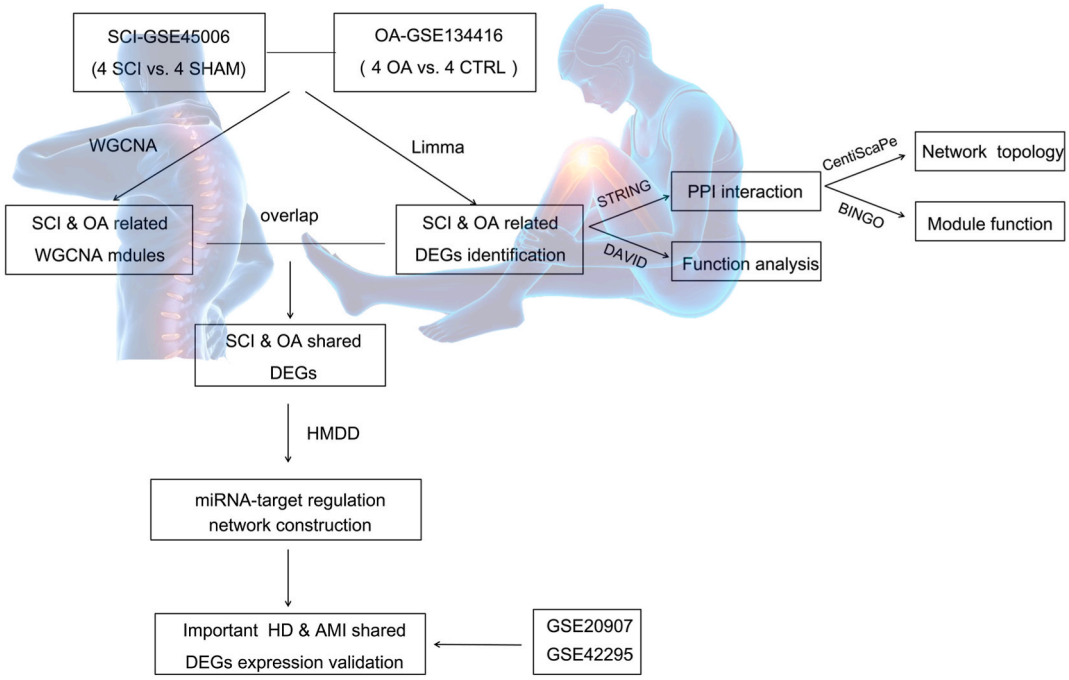

Fig. 1. Overall study design.

biological processes mainly contained "extracellular matrix organization," "cell adhesion," "response to hypoxia," "inflammatory response," "response to lipopolysaccharide," "positive regulation of apoptotic process," and "positive regulation of cell migration," which included 13 (*MMP2*, *MMP14*, *POSTN*, etc.), 16 (*CX3CR1*, *POSTN*, *B4GALT1*, etc.), 14 (*POSTN*, *BNIP3*, *MMP2*, etc.), 14 (*CX3CR1*, *STK39*, *IL18*, etc.), 12 (*CASP3*, *CCL2*, *LY96*, etc.), 13 (*B4GALT1*, *TNFRSF12A*, *MMP2*, etc.), and 12 genes (*MMP14*, *GPNMB*, *MYOC*, etc.), respectively (Table 2). In addition, KEGG pathways showed that these identified DEGs were significantly enriched in "Toll-like receptor signaling pathway," "TNF signaling pathway," "NF-kappa B signaling pathway," "chemokine signaling pathway," "phagosome," and "cytokine-cytokine receptor interaction," which contained six genes (*CTSK*, *CCL4*, *CCL3*, *LY96*, *FOS*, and *LBP*), six genes (*MMP14*, *CASP3*, *BCL3*, *CCL2*, *FOS*, and *JUNB*), five genes (*PLAU*, *CCL4*, *LY96*, *LBP*, and *GADD45G*), seven genes (*CX3CR1*, *CCL7*, *CCL4*, *CCL3*, *CCL2*, *CCR5*, and *CXCL14*), nine genes (*SEC61A1*, *TUBB6*, *CLEC7A*, etc.), and 11 genes (*CX3CR1*, *TNFRSF12A*, *CCL7*, etc.), respectively (Table 2).

3.2. Three modules extracted from the PPI network

We obtained 731 PPIs (confidence score >0.4) for 185 common DEGs from the STRING database and used them to construct a PPI network. As shown in Fig. 3A, the network included 169 nodes. The topological parameters of the top 20 nodes are shown in Table 3; Ccl2 (degree = 42), Timp1 (degree = 41), Mmp2 (degree = 38), Igf (degree = 37), and Cd44 (degree = 36) had the highest degrees.

Subsequently, we obtained three network modules (degree cutoff = 2, node score cutoff = 0.2, and K-core = 2) by applying the Mcode plugin, which contained 44 DEGs (gene set 1). Module 1 had 30 upregulated genes, module 2 had six upregulated genes and one downregulated gene, and module 3 had 10 upregulated genes (Fig. 3B). The three modules were significantly enriched in 30, 27, and 55 GO biological processes, respectively.

3.3. SCI and OA-related WGCNA network modules

WGCNA network analysis was conducted to cluster genes into modules to identify SCI- and OA-related modules using GSE45006 and GSE103416, respectively. Consequently, eight SCI-related-and seven OA-related modules were obtained. Subsequently, with a correlation coefficient (r) > 0.3 as the cutoff, we retained the brown module (r = 0.55, $p = 0$), turquoise module (r = 0.96, $p = 0$), and yellow module (r = 0.55, $p = 0$) for SCI, and turquoise module (r = 0.97, $p = 0$) and green module (r = 0.31, $p = 1e\text{-}126$) for OA (Fig. 4A and B). As shown in Fig. 4C and 634 common signature genes were shared by positively correlated modules of SCI and OA (gene set 2). Consequently, by considering the intersection of gene sets 1 and 2, we obtained 43 overlapping genes (gene set 3; Table 4).

3.4. Construction of common miRNA-target gene-pathway network

From the HMDD database (version 3.2), we extracted 44 SCI-related and 61 OA-related miRNAs, 17 of which were shared between

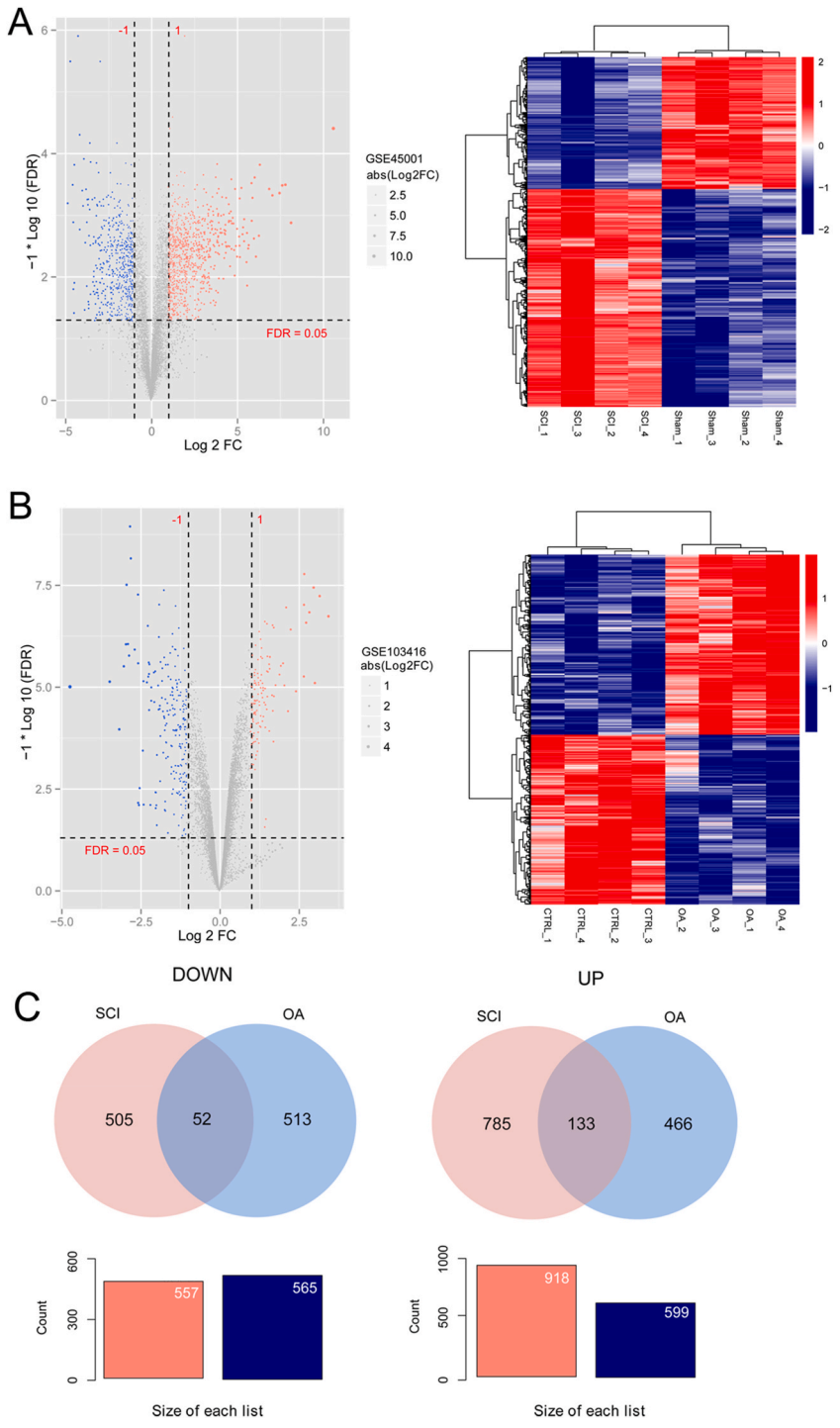

Fig. 2. Identification of common differentially expressed genes (DEGs) between SCI and OA. (A) Volcano plot and heatmaps of DEGs in SCI (A) and OA (B). (C) Venn diagram of the common upregulated and downregulated genes between SCI and OA. Count represents the number of genes.

both diseases. The target genes of each shared miRNA were predicted using the miRWalk database (version 3.0). Overlapping genes between the predicted target genes and gene set 3 were retained. Consequently, we acquired eight miRNA-target gene pairs, including six miRNAs (miR-125b-5p, miR-130a-3p, miR-16-5p, miR-204-5p, miR-204-3p, and miR-30b-3p) and five genes (cluster of differentiation-44 (*CD44*), transforming growth factor-beta receptor 1 (*TGFBR*1), CC chemokine receptor 5 (*CCR5*), C-type lectin domain family 7 member A (*CLEC7A*), and insulin-like growth factor 1 (*IGF1*)).

Table 2
Significant GO biological processes and KEGG signaling pathways for the common DEGs in SCI and OA.

Category	Term	Count	PValue	FDR	Genes
GOTERM_BP_DIRECT	GO:0030198~extracellular matrix organization	13	8.60E-08	1.40E-04	POSTN, B4GALT1, MMP2, TNFRSF11B, MMP12, LGALS3, MMP14, COL5A1, ADAMTS1, COL5A3, COL5A2, BCL3, MMP19
GOTERM_BP_DIRECT	GO:0007155~cell adhesion	16	1.31E-06	8.99E-04	CX3CR1, POSTN, B4GALT1, TNFRSF12A, PRKCE, COL12A1, LSAMP, THBS2, THBS4, VCAN, GPNMB, COL5A1, PDPN, SDC1, MFGE8, CD44
GOTERM_BP_DIRECT	GO:0031663~lipopolysaccharide-mediated signaling pathway	7	1.65E-06	8.99E-04	PRKCE, CD180, CCL3, IL18, CCL2, LY96, LBP
GOTERM_BP_DIRECT	GO:0001666~response to hypoxia	14	2.67E-06	1.09E-03	POSTN, BNIP3, MMP2, IL18, IGF1, HK2, TGFBR1, MMP12, MMP14, PLAU, CASP3, CCL2, HMOX1, SOX4
GOTERM_BP_DIRECT	GO:0048245~eosinophil chemotaxis	5	1.16E-05	3.07E-03	LGALS3, CCL7, CCL4, CCL3, CCL2
GOTERM_BP_DIRECT	GO:0048246~macrophage chemotaxis	5	1.16E-05	3.07E-03	CX3CR1, LGALS3, MMP2, CCL3, CCL2
GOTERM_BP_DIRECT	GO:0006954~inflammatory response	14	1.37E-05	3.07E-03	CX3CR1, STK39, IL18, TCIRG1, CCL7, PDPN, CCL4, CCL3, SDC1, CCL2, OLR1, S1PR3, CCR5, CD44
GOTERM_BP_DIRECT	GO:2000503~positive regulation of natural killer cell chemotaxis	4	1.50E-05	3.07E-03	CCL7, CCL4, CCL3, CXCL14
GOTERM_BP_DIRECT	GO:0061760~antifungal innate immune response	5	2.41E-05	4.38E-03	CX3CR1, CLEC4A, CLEC4A1, CLEC4A3, CLEC7A
GOTERM_BP_DIRECT	GO:0032496~response to lipopolysaccharide	12	5.53E-05	8.20E-03	CASP3, CCL2, LY96, IGF1, FOS, LBP, CCR5, LITAF, LOXL1, TIMP4, SNCA, ABCG2
GOTERM_BP_DIRECT	GO:0030335~positive regulation of cell migration	12	5.53E-05	8.20E-03	MMP14, GPNMB, MYOC, CCL7, CLEC7A, PLAU, MMP2, PDPN, ITGAX, CCL3, IGF1, TGFBR1
GOTERM_BP_DIRECT	GO:0071560~cellular response to transforming growth factor beta stimulus	8	6.34E-05	8.62E-03	CX3CR1, POSTN, CTSK, PDE2A, FOS, CCR5, TGFBR1, RUNX1
GOTERM_BP_DIRECT	GO:0071222~cellular response to lipopolysaccharide	12	8.60E-05	1.08E-02	CX3CR1, SBNO2, PLAU, CD180, PDE2A, IL18, CCL2, LY96, LBP, CCR5, CD68, LITAF
GOTERM_BP_DIRECT	GO:0032720~negative regulation of tumor necrosis factor production	7	1.02E-04	1.19E-02	CLEC4A, CLEC4A3, GPNMB, BCL3, IGF1, LBP, LILRB4
GOTERM_BP_DIRECT	GO:0042542~response to hydrogen peroxide	7	1.17E-04	1.26E-02	GNAO1, NR4A3, MMP2, CASP3, OLR1, SDC1, HMOX1
GOTERM_BP_DIRECT	GO:0032760~positive regulation of tumor necrosis factor production	8	1.23E-04	1.26E-02	CLEC7A, CCL4, CCL3, IL18, CCL2, LY96, LBP, CCR5
GOTERM_BP_DIRECT	GO:0030199~collagen fibril organization	6	1.50E-04	1.44E-02	COL5A1, LUM, COL5A2, SERPINH1, LOXL1, TGFBR1
GOTERM_BP_DIRECT	GO:0070098~chemokine-mediated signaling pathway	6	1.93E-04	1.66E-02	CX3CR1, CCL7, CCL4, CCL3, CCL2, CCR5
GOTERM_BP_DIRECT	GO:0014070~response to organic cyclic compound	12	2.02E-04	1.66E-02	MMP12, GNAO1, MMP14, LUM, CTSK, CASP3, SERPINH1, IGF1, FOS, JUNB, TGFBR1, CD44
GOTERM_BP_DIRECT	GO:0002548~monocyte chemotaxis	5	2.04E-04	1.66E-02	LGALS3, CCL7, CCL4, CCL3, CCL2
GOTERM_BP_DIRECT	GO:0030574~collagen catabolic process	5	2.31E-04	1.79E-02	MMP12, MMP14, MMP2, CTSK, MMP19
GOTERM_BP_DIRECT	GO:0043065~positive regulation of apoptotic process	13	3.36E-04	2.49E-02	B4GALT1, TNFRSF12A, BNIP3, MMP2, IL18, TGFBR1, IGF2R, GADD45G, CASP3, HMOX1, CTSD, SOX4, GPLD1
GOTERM_BP_DIRECT	GO:0007568~aging	12	3.83E-04	2.62E-02	GNAO1, MMP2, CCL2, IGF1, FOS, TIMP1, CCR5, CD68, LITAF, TGFBR1, SNCA, ABCG2
GOTERM_BP_DIRECT	GO:0071356~cellular response to tumor necrosis factor	9	3.85E-04	2.62E-02	POSTN, CCL7, CTSK, CCL4, CCL3, IL18, CCL2, FOS, CCR5
GOTERM_BP_DIRECT	GO:0001649~osteoblast differentiation	7	4.02E-04	2.62E-02	GPNMB, MYOC, CCL3, IL18, IGF1, JUNB, CTHRC1
GOTERM_BP_DIRECT	GO:0042060~wound healing	8	5.03E-04	3.16E-02	POSTN, B4GALT1, PLAU, CASP3, SDC1, IGF1, TIMP1, TSKU
GOTERM_BP_DIRECT	GO:0030593~neutrophil chemotaxis	6	6.41E-04	3.87E-02	LGALS3, CCL7, CCL4, CCL3, CCL2, LBP
GOTERM_BP_DIRECT	GO:0009612~response to mechanical stimulus	7	6.86E-04	3.93E-02	MMP14, POSTN, MMP2, CCL2, IGF1, FOS, JUNB
GOTERM_BP_DIRECT	GO:0055093~response to hyperoxia	5	7.07E-04	3.93E-02	PLAU, BNIP3, MMP2, PDPN, IL18
GOTERM_BP_DIRECT	GO:0006508~proteolysis	13	7.23E-04	3.93E-02	C1S, MMP2, PCOLCE, MMP12, MMP14, PLAU, ADAMTS1, CTSK, CASP3, MMP19, NRIP3, MASP1, CTSD
GOTERM_BP_DIRECT	GO:0001501~skeletal system development	7	7.52E-04	3.95E-02	LGALS3, MMP14, VCAN, COL5A2, TGFBR1, SOX4, RUNX1

(*continued on next page*)

Table 2 (*continued*)

Category	Term	Count	PValue	FDR	Genes
KEGG_PATHWAY	rno04060:Cytokine-cytokine receptor interaction	11	1.08E-06	8.72E-04	CX3CR1, TNFRSF12A, CCL7, CCL4, CCL3, IL18, CCL2, TNFRSF11B, CCR5, CXCL14, TGFBR1
KEGG_PATHWAY	rno04145:Phagosome	9	1.38E-06	1.12E-03	SEC61A1, TUBB6, CLEC7A, OLR1, SEC61B, TCIRG1, THBS2, FCGR1A, THBS4
KEGG_PATHWAY	rno04380:Osteoclast differentiation	7	2.95E-06	2.39E-03	CTSK, TNFRSF11B, FOS, FCGR1A, JUNB, LILRB4, TGFBR1
KEGG_PATHWAY	rno05323:Rheumatoid arthritis	6	3.44E-06	2.79E-03	CTSK, CCL3, IL18, CCL2, TCIRG1, FOS
KEGG_PATHWAY	rno04512:ECM-receptor interaction	6	3.62E-06	2.93E-03	COL6A2, SDC1, COL6A3, THBS2, THBS4, CD44
KEGG_PATHWAY	rno04620:Toll-like receptor signaling pathway	6	4.83E-06	3.91E-03	CTSK, CCL4, CCL3, LY96, FOS, LBP
KEGG_PATHWAY	rno04142:Lysosome	7	4.90E-06	3.97E-03	GLB1, CTSK, TCIRG1, CD68, LITAF, CTSD, IGF2R
KEGG_PATHWAY	rno00052:Galactose metabolism	4	6.72E-06	5.44E-03	B4GALT1, GLB1, HK2, AKR1B8
KEGG_PATHWAY	rno04974:Protein digestion and absorption	6	7.45E-06	6.03E-03	COL5A1, COL6A2, COL5A3, COL5A2, COL12A1, COL6A3
KEGG_PATHWAY	rno04668:TNF signaling pathway	6	1.02E-05	8.23E-03	MMP14, CASP3, BCL3, CCL2, FOS, JUNB
KEGG_PATHWAY	rno05205:Proteoglycans in cancer	8	1.08E-05	8.74E-03	FZD1, PLAU, LUM, MMP2, CASP3, SDC1, IGF1, CD44
KEGG_PATHWAY	rno05417:Lipid and atherosclerosis	8	1.13E-05	9.19E-03	CASP3, CCL3, IL18, OLR1, CCL2, LY96, FOS, LBP
KEGG_PATHWAY	rno04062:Chemokine signaling pathway	7	2.06E-05	1.67E-02	CX3CR1, CCL7, CCL4, CCL3, CCL2, CCR5, CXCL14
KEGG_PATHWAY	rno05202:Transcriptional misregulation in cancer	7	2.73E-05	2.21E-02	NR4A3, PLAU, TSPAN7, IGF1, FCGR1A, RUNX1, GADD45G
KEGG_PATHWAY	rno04064:NF-kappa B signaling pathway	5	3.03E-05	2.45E-02	PLAU, CCL4, LY96, LBP, GADD45G
KEGG_PATHWAY	rno04210:Apoptosis	5	5.77E-05	4.67E-02	CTSK, CASP3, FOS, CTSD, GADD45G

These DEGs were significantly enriched in six signaling pathways, whereas these miRNAs were significantly involved in 23 signaling pathways ($p < 0.05$), according to the mirPathv3 database. Six overlapping signaling pathways, together with six miRNAs and five genes, were used to construct the miRNA-gene-pathway regulatory network, including the forkhead box O (FoxO) signaling pathway, proteoglycans in cancer, endocytosis, mitogen-activated protein kinase (MAPK) signaling pathway, cytokine-cytokine receptor interaction, and cancer pathways (Fig. 5A). As shown in Fig. 5A, CD44 expression was regulated by miR-125b-5p, miR-16-5p, and miR-204-3p. Endocytosis and FoxO signaling pathways were significantly associated with all six miRNAs. These five genes are regarded as key common genes in SCI and OA.

3.5. Establishment of TF regulatory network and immune analysis

A total of 68 connection pairs were obtained in the TF regulatory network (Fig. 5B), and *FOS* and *HMOX1* were linked with more TFs (including *TRP3*, *ELK1*, *CREBBP*, and *NFE2L2*) compared with the other DEGs. Based on this network, we observed that the TFs of *SMARCA2* and *TCF4* activated the expression of *CD44* as well as *ESR1* activated *IGF1* expression, and *HTATIP2* repressed the expression of IGF1 (Fig. 5B).

After immune analysis, five types of immune cells were significantly infiltrated in SCI ($p < 0.05$), including B cells, $CD4^+$ T cells, macrophages, neutrophils, and myeloid dendritic cells (mDCs); in OA, three types of immune cells were significantly infiltrated, including B cells, $CD4^+$ T cells, and mDCs ($p < 0.05$, Fig. 5C). The shared significantly different distributions of immune cells between SCI and OA were B cells, $CD4^+$ T cells, and mDCs, while macrophages and neutrophils were unique in SCI. The correlations between the five important DEGs and the significantly different distributions of immune cells in SCI and OA were calculated. In SCI, *CCR5* was significantly negatively correlated with $CD4^+$ T cells and macrophages ($p < 0.05$), whereas *CD44*, *CLEC7A*, *IGF1*, and *TGFBR1* were all significantly positively correlated with the five types of immune cells with significantly different distributions ($p < 0.05$, Fig. 5D). In OA, the five important DEGs (*CCR5*, *CD44*, *CLEC7A*, *IGF1*, and *TGFBR1*) were significantly negatively associated with B cells and $CD4^+$ T cells ($p < 0.05$), whereas all were positively associated with mDCs ($p < 0.05$, Fig. 5D).

3.6. Verification of the identified DEGs in the validation datasets and rat tissue samples

In the discovery cohorts (GSE45006 and GSE103416), we found that *CD44*, *TGFBR1*, *CCR5*, *CLEC7A,* and *IGF1* were all significantly upregulated in both SCI and OA samples compared with control samples ($p < 0.005$, Fig. 6A). The expression of the five identified DEGs was analyzed in validation cohorts (GSE20907 and GSE42295) and rat tissue samples. In GSE20907, the *CCR5* and *TGFBR1* expression was significantly upregulated in SCI compared with the control samples ($p < 0.05$), while in GSE42295, the expression

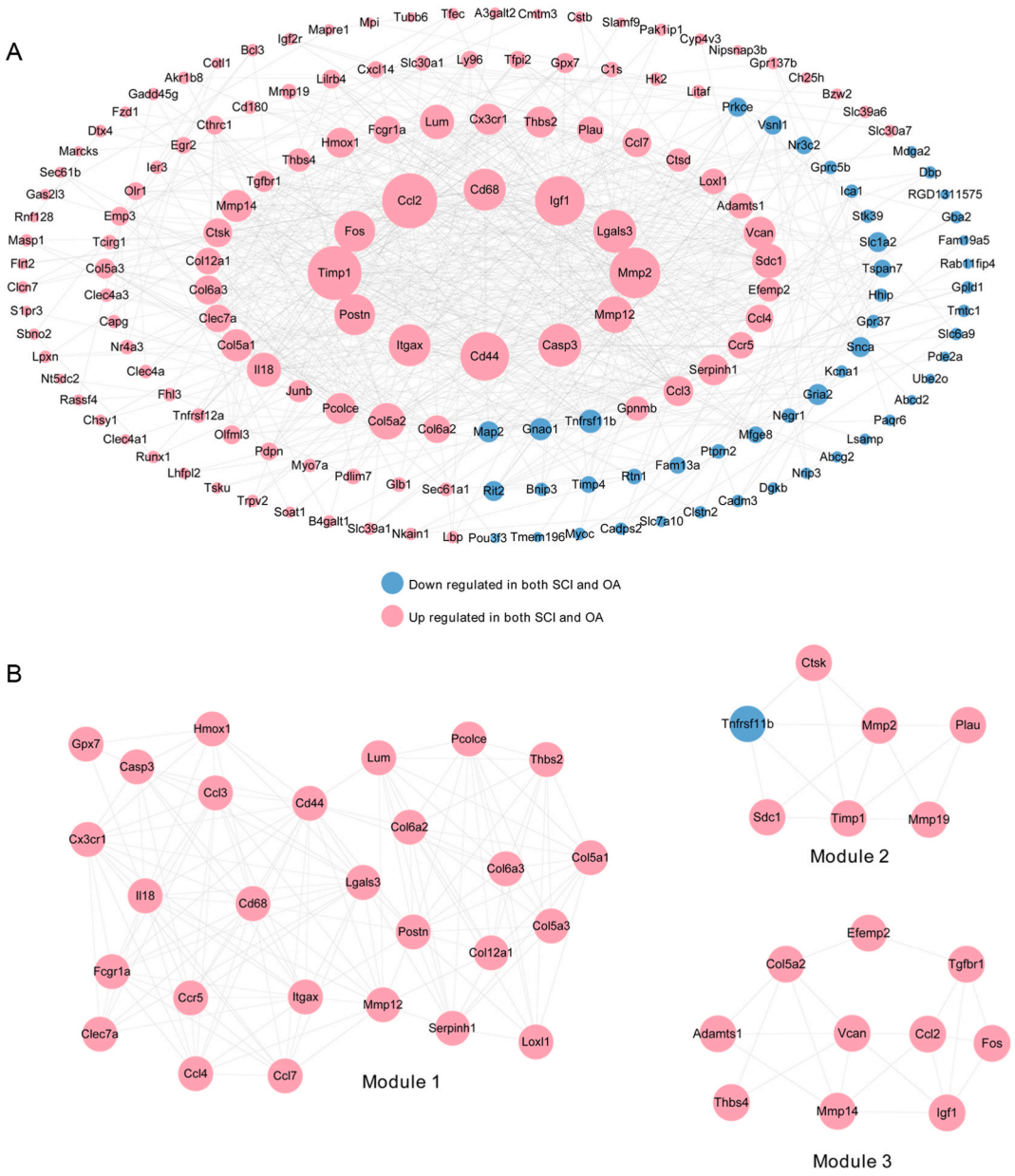

Fig. 3. Protein-protein interactions (PPI) among DEGs. (A) A PPI network was constructed. (B) Three modules extracted from the PPI network. Blue and red nodes stand for down and upregulated genes, respectively. Node size represents the degree of a specific node. A link between two nodes represents the interaction between two proteins. (For interpretation of the references to colour in this figure legend, the reader is referred to the Web version of this article.)

levels of *CD44*, *TGFBR1*, *CCR5*, and *CLEC7A* were higher in OA samples than in the control samples ($p < 0.05$, Fig. 6B). In the rat tissue samples, we also observed that compared with the control group, four of the five genes were significantly upregulated in the SCI tissue samples ($p < 0.05$), and the five identified DEGs were significantly upregulated in the OA tissue samples ($p < 0.05$, Fig. 6C). Related miRNAs were analyzed using RT-qPCR. Except for miR-30b-3p, the levels of miR-125b-5p, miR-130a-3p, miR-16-5p, miR-204-5p, and miR-204-3p were significantly lower in the SCI and OA groups than in the control group (p-value <0.05; Fig. 6D). These results indicated that the consistency rates in the RT-qPCR and bioinformatics-based expression analyses of DEGs and miRNAs were 80 % and 83.33 %, respectively, implying high relative reliability of the bioinformatics results.

4. Discussion

SCI is strongly associated with OA in clinical practice, resulting in a high incidence of disability and socioeconomic costs [9].

Table 3
Node topology information of protein-protein interaction network.

name	AverageShortes tPathLength	Betweenness Centrality	Closeness Centrality	Degree
Ccl2	2	0.10942875	0.5	42
Timp1	1	0.30196212	1	41
Mmp2	1.1875	0.55975967	0.84210526	38
Igf1	1.71698113	1.05122062	0.58241758	37
Cd44	2.14705882	0.41345196	0.46575342	36
Casp3	2.07627119	0.25789525	0.48163265	31
Lgals3	1.62962963	0.70779912	0.61363636	31
Cd68	2.11627907	0.23038544	0.47252747	30
Itgax	1.72727273	0.78778405	0.57894737	30
Postn	1.33333333	0.16838037	0.75	29
Fos	2.01351351	1.49738119	0.4966443	29
Mmp12	1.55555556	0.32248947	0.64285714	25
Col5a2	2.66315789	0.74394372	0.37549407	25
Sdc1	1.375	0.08477356	0.72727273	23
Lum	1.47826087	0.18781264	0.67647059	23
Il18	1.91666667	0.23661417	0.52173913	23
Vcan	0	0	0	21
Col5a1	3.16666667	0.47272803	0.31578947	21
Mmp14	1.42105263	0.12385881	0.7037037	21
Thbs2	1.28571429	0.09010671	0.77777778	20

Patients with SCI are more prone to OA [5]. *CXCL10* is upregulated in SCI [39,40], and the CXCR3/CXCL10 axis is associated with SCI and OA development [39,41]. However, limited information is available on the co-occurrence of SCI and OA. The current study focused on deciphering the common molecular mechanisms underlying SCI and OA using comprehensive bioinformatics analyses. In this study, 185 common DEGs were identified in the pathogenesis of SCI and OA, and three hub modules were extracted from the constructed PPI network. Three SCI-related and two OA-related modules were identified using WGCNA, and 43 overlapping genes were identified. Subsequently, a regulatory network composed of six common miRNAs, five common target genes, and six significant signaling pathways was constructed. The six significant signaling pathways included proteoglycans in cancer, endocytosis, cytokine-cytokine receptor interactions, pathways in cancer, MAPK signaling, and FoxO signaling. Proteoglycan is an important component of the extracellular matrix, providing biomechanical properties essential for its proper functioning, and is a key participant in cartilage diseases, especially in the degradation of the extracellular matrix [42]. These results indicate that proteoglycans are closely associated with OA and SCI progression. Feng et al. [43] reported that cytokine-cytokine receptor interactions and T-cell receptor signaling pathways were significantly upregulated in OA. Endocytosis is a process by which cells actively internalize molecules and surface proteins through endocytic vesicles and is associated with OA progression [44]. The MAPK signaling pathway is involved in inducing cell senescence, chondrocyte differentiation, matrix metalloproteinase synthesis, and pro-inflammatory factor production, all of which are associated with the pathogenesis of OA [45]. Tian et al. [46] also showed that umbilical cord stem cells can repair SCI in rats via the MAPK signaling pathway. Oxidative stress plays an important role in the pathogenesis of SCI and OA. The FoxO signaling pathway is associated with oxidative stress [47]. It can be inferred that the proteoglycan pathways in cancer, endocytosis, cytokine-cytokine receptor interactions, MAPK, and FoxO may participate in the occurrence and development of SCI and OA. However, their specific roles in SCI and OA need to be explored in future studies.

In the constructed miRNA-gene-pathway network, *CD44*, *TGFBR1*, *CCR5*, *CLEC7A*, and *IGF1* were identified as the important signature genes, and it was found that *CD44, TGFBR1, CCR5*, and *IGF1* were significantly upregulated in the SCI tissue samples, and the five identified DEGs were significantly upregulated in the OA tissue samples. *CD44*, a cell adhesion molecule, plays an essential role in modulating leukocyte adhesion and migration [48]. Upregulated *CD44* expression was found in the damaged articular cartilage of patients with OA and in the SCI rat model, which is in concordance with our results [49]. Our TF regulatory network showed that *SMARCA2* and *TCF4* activated the expression of *CD44*; however, the effects of *SMARCA2* and *TCF4* on *CD44* should be further verified. TGFBR1 is an established key receptor of the immune-modulatory TGFB1 signaling pathway involved in the neuronal regenerative mechanism following SCI [50]. TGFBR may inhibit OA progression during aging [51]. CC chemokine receptor 5 is expressed on the surface of immune cells (monocytes, macrophages, activated T cells, and NK cells) and participates in the recruitment of immune cells to inflammation sites. Suppression *CCR5* facilitates SCI-related locomotor recovery in mice models [52]. *CCR5* ablation inhibits cartilage degeneration during the development of post-traumatic OA [53]. Moreover, *CCR5* blockade alleviates neuropathic pain and has been suggested as an innovative therapeutic strategy [54]. *CLEC7A*, namely dectin1, is expressed by macrophages and other immune cells [55]. A recent study reported that *CLEC7A* is a diagnostic signature gene in patients with OA [56]. IGF1 plays an important role in many aspects of growth, development, and metabolism and is mediated by the IGF1 receptor, whose function is related to the MAPK and phosphoinositide 3-kinase signaling pathways [57]. A previous study showed that IGF1 overexpression could improve the survival rate of stem cells and promote the recovery of nerve function after SCI [58]. Another study showed that cartilage-specific *SIRT6* deficiency increases the severity of OA in mice by inhibiting IGF1 [59]. Our results showed that *ESR1* activates *IGF1* expression, whereas *HTATIP2* repressed the expression of *IGF1*. Together with our results, these reports suggest that *CD44*, *TGFBR*1, *CCR5*, and *IGF1* are shared molecular biomarkers and promising therapeutic targets in SCI and OA.

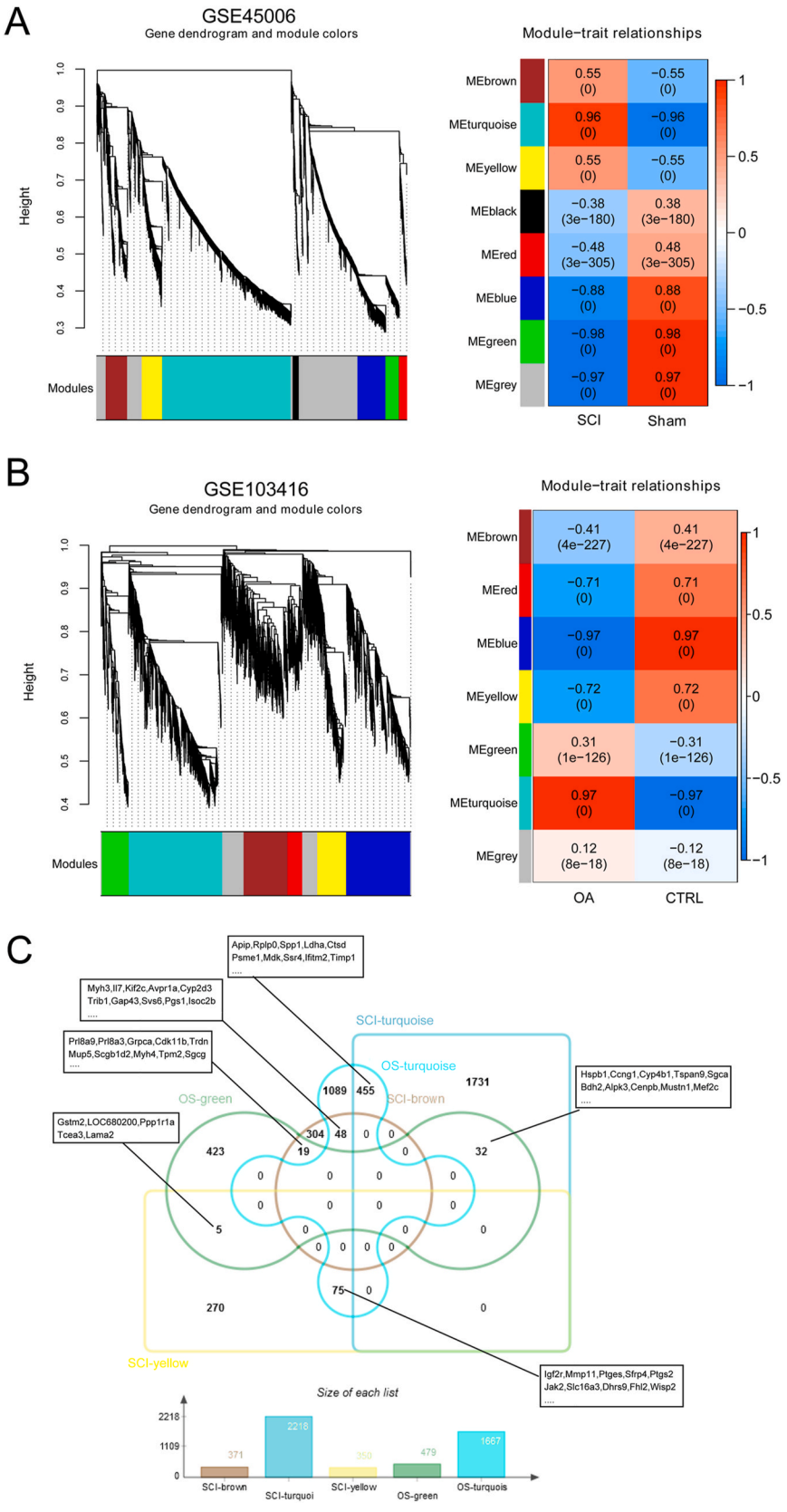

(caption on next page)

Fig. 4. WGCNA network analysis. (A) Cluster dendrogram and module-trait relationships in SCI (GSE45006). (B) Cluster dendrogram and module-trait relationships in OA (GSE103416). (C) Analysis of the shared genes between three SCI-related modules and two OS-related modules.

Table 4
The 43 overlapped genes in gene set 3.

Gene symbol	GSE45006		GSE103416	
	FDR	logFC	FDR	logFC
Adamts1	2.62E-03	2.040143	0.005557	1.801482
Casp3	2.65E-02	1.613434	0.00794	1.145859
Ccl2	1.52E-04	6.420283	0.002537	1.884328
Ccl3	2.29E-04	1.534402	0.004825	1.586507
Ccl4	9.90E-03	3.017314	0.0125	1.199681
Ccl7	1.54E-02	1.524259	0.00157	3.209442
Ccr5	4.09E-02	1.37823	0.008708	1.658978
Cd44	2.94E-03	2.509303	0.008342	1.0712
Cd68	1.33E-03	8.255697	0.006231	1.395853
Clec7a	5.77E-03	5.63262	0.042423	1.275015
Col12a1	3.99E-02	1.943092	0.000408	2.246732
Col5a1	2.87E-02	2.002988	0.014656	1.09525
Col5a2	3.07E-03	2.97501	0.0052	1.205014
Col5a3	1.61E-03	1.465275	0.000942	1.832335
Col6a2	1.21E-02	3.384046	0.010298	1.078639
Col6a3	2.75E-03	4.401078	0.002376	1.37552
Ctsk	9.32E-04	4.618641	0.005383	1.521575
Cx3cr1	1.25E-02	1.264628	0.002737	1.780696
Efemp2	1.92E-03	4.181263	0.012806	1.127108
Fcgr1a	2.54E-03	3.138032	0.047525	1.002116
Fos	3.23E-02	1.463319	0.006397	1.502521
Gpx7	8.03E-03	1.830792	0.029318	1.02613
Hmox1	4.76E-03	5.243781	0.002138	1.908782
Igf1	5.71E-04	2.636773	0.00739	1.0546
Il18	2.85E-03	1.752243	0.030085	1.053536
Itgax	2.80E-02	2.180905	0.020316	1.095645
Lgals3	6.46E-03	2.352598	0.008009	1.371294
Loxl1	2.37E-02	2.81465	0.004506	1.227315
Lum	5.37E-03	3.234917	0.001917	1.406198
Mmp12	1.23E-03	5.941201	0.00032	4.000497
Mmp14	8.17E-03	2.11305	0.000392	1.959506
Mmp19	9.45E-04	1.97182	0.001906	1.76592
Mmp2	5.35E-04	5.231318	0.001917	1.337119
Pcolce	1.70E-02	3.255378	0.008775	1.059503
Plau	1.02E-03	4.136138	0.003925	1.661092
Postn	1.94E-03	5.663375	0.001514	1.632114
Sdc1	2.49E-03	3.092865	0.00949	1.423815
Serpinh1	1.36E-02	1.006211	0.013866	1.09171
Tgfbr1	9.06E-03	2.118774	0.030619	1.037802
Thbs2	2.46E-03	3.467432	0.002439	1.355989
Thbs4	4.01E-02	1.598017	0.005666	1.510782
Timp1	9.71E-03	3.093405	0.001448	1.730227
Vcan	2.81E-02	1.330399	0.002886	1.595628

FDR, false discovery rate; FC, fold change.

The five crucial target DEGs in the miRNA-gene-pathway network were regulated by six miRNAs: miR-125b-5p, miR-130a-3p, miR-16-5p, miR-204-5p, miR-204-3p, and miR-30b-3p. RT-qPCR validation showed that in addition to miR-30b-3p, the levels of the remaining miRNAs were significantly lower in the SCI and OA groups. miR-125b-5p negatively regulates the expression of inflammatory genes in human OA chondrocytes [60]. Downregulation of miR-130a-3p improves SCI-induced neuropathic pain [61]. Multiple studies show that miR-130a-3p is implicated in the progression of OA and suppresses chondrocyte autophagy [62,63]. miR-130a-3p is a well-defined upstream regulator of *TGFBR1* [64]. Consistently, the miRNA-gene-pathway network showed that miR-130a-3p regulates downstream TGFBR1. Therefore, miR-130a-3p/TGFBR1 signaling may play an important role in SCI and OA. miR-16-5p expression is increased in SCI mouse models, decreases cell viability, and promotes inflammation and oxidative stress [65]. Moreover, miR-16-5p knockdown suppresses neuronal apoptosis and inflammation caused by SCI by activating the MAPK pathway [66], which is in agreement with our finding that miR-16-5p is significantly related to the MAPK pathway. miR-204-5p may ameliorate neuropathic pain and inhibit inflammation [67]. Bioinformatics analysis suggested that miR-204-5p may be a potential biomarker of SCI [68]. miR-204-5p regulates downstream *CCR5* [69] and suppresses synovial fibroblast inflammation in OA [70]. Moreover, growing evidence supports the negative role of miR-204-5p in the progression of OA [71,72]. These studies are in concordance with our findings that miR-204-5p targets *CCR5* in the regulatory network and is a common mechanism in SCI and OA. Therefore, we hypothesized that miR-125b-5p, miR-130a-3p, miR-16-5p, miR-204-5p, and miR-204-3p may be involved in the progression of SCI and

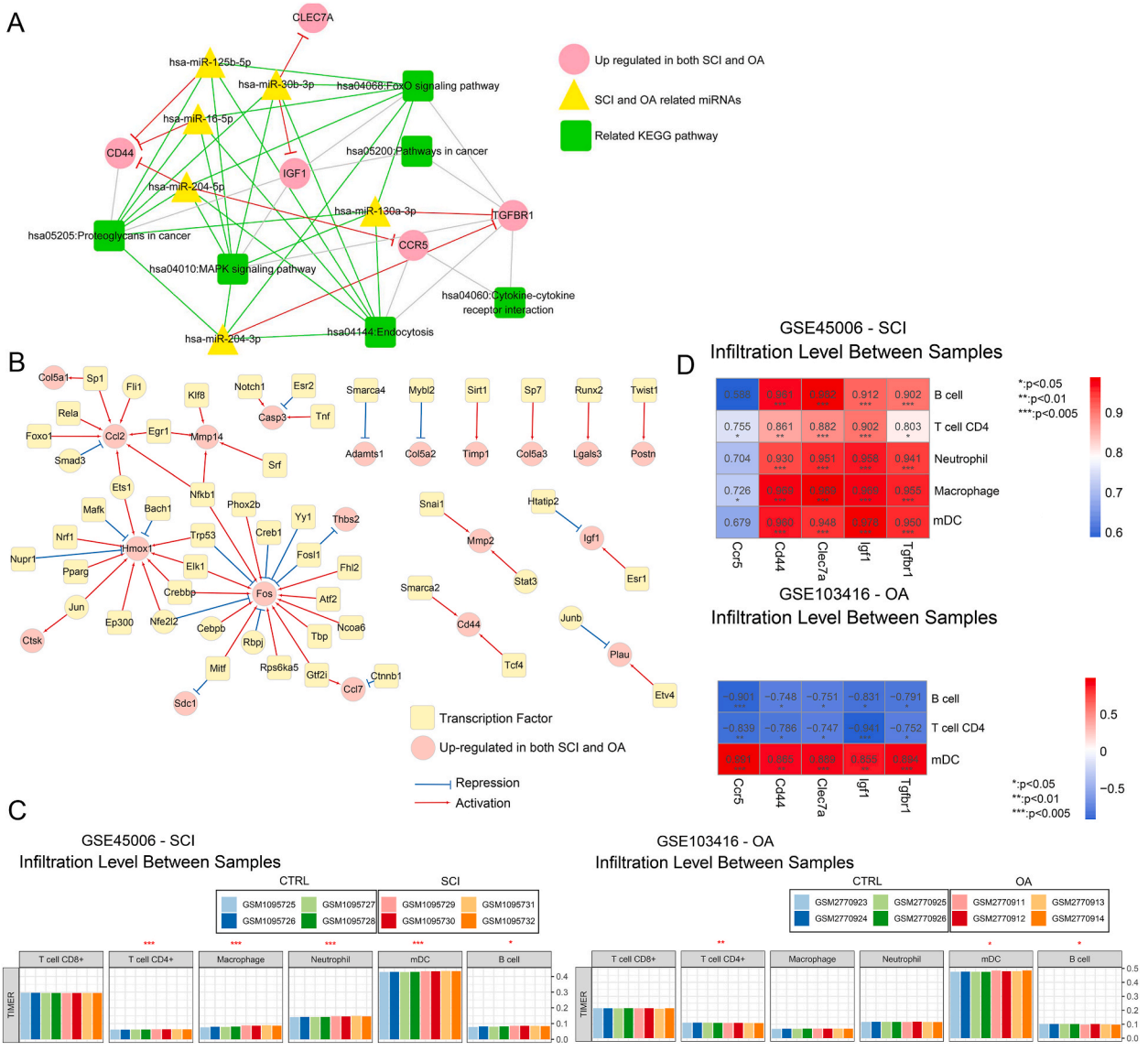

Fig. 5. The construction of the miRNA-gene-pathway network and transcriptional factors (TFs) regulatory network, and immune analysis. (A) The miRNA-gene-pathway network based on the five important DEGs. Red links represent correlations between miRNAs and target genes. Green and grey links denote significant enrichments of miRNAs and DEGs in KEGG pathways, respectively. (B) The TFs regulatory network of the 43 identified DEGs. Red and blue links represent activation and repression, respectively. The red circles denote the up-regulate genes both in SCI and OA; and the yellow squares denote the TFs. (C) The proportion of each type of immune cells in each sample in SCI and OA. (D) The correlation heatmaps between the five important DEGs and the significantly different distribution of immune cells in SCI and OA. (For interpretation of the references to colour in this figure legend, the reader is referred to the Web version of this article.)

OA and may be potential therapeutic targets for both SCI and OA.

However, this study has some limitations. First, the datasets used had a limited sample size, and further experiments need to be conducted with larger sample sizes. Second, signature expression differences between specific cell populations should be evaluated to analyze the heterogeneity between cell types and regions within SCI and OA samples. Third, the relationships between the associated gene/miRNA expression levels and the quantified metrics of injury severity or OA progression should be analyzed in the future using more data. Additionally, in vitro functional studies involving the knockdown or overexpression of some of the identified signature genes and miRNAs in cell line models should be conducted to elucidate their specific mechanistic roles in SCI and OA pathology.

5. Conclusion

Our study suggests a miRNA-target gene-pathway network that depicts possible common mechanisms of SCI and OA based on

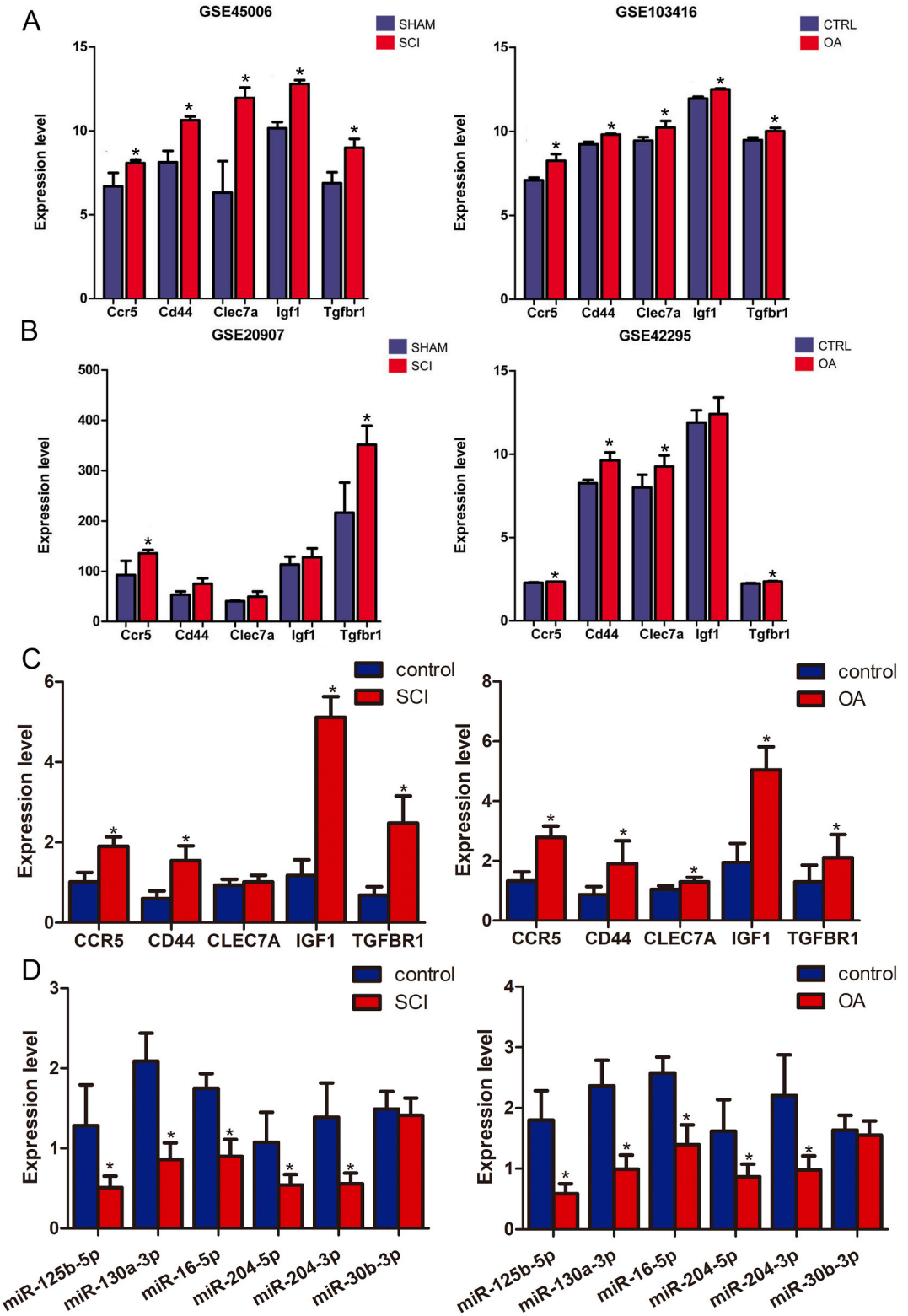

Fig. 6. Expression levels of the five identified key DEGs and their related miRNAs. (A) The expression of the five identified DEGs in the discovery cohorts (GSE45006, and GSE103416). (B) The expression of the five identified DEGs in the validation cohorts (GSE20907, and GSE42295). (C) The expression of the five identified DEGs in the SCI and OA tissue samples. (D) The levels of the related miRNAs in the SCI and OA tissue samples. * $0.01 < p < 0.05$, ** $0.005 < p < 0.01$, ***$p < 0.005$.

shared gene signatures, miRNAs, and signaling pathways from comprehensive bioinformatics analysis. *CD44*, *TGFBR1*, *CCR5*, and *IGF1*, and their related miRNAs (miR-125b-5p, miR-130a-3p, miR-16-5p, miR-204-5p, and miR-204-3p) may serve as promising biomarkers and candidate therapeutic targets for SCI and OA. Our study advances knowledge concerning the common regulatory mechanisms of SCI and OA and may have important implications for patients with concurrent SCI and OA.

Ethics approval and consent to participate

All animal experiments were conducted in accordance with the National Medical Advisory Committee guidelines and approved by the Animal Care and Use Committee of Shanghai Ninth People's Hospital, Shanghai Jiao Tong University School of Medicine.

Consent for publication

Not applicable.

Availability of data and materials

The data that support the findings of this study are available from Gene Expression Omnibus (GEO) database (http://www.ncbi.nlm.nih.gov/geo/) with accession numbers of GSE45006, GSE20907, GSE103416 and GSE42295.

Funding

This study was funded by the Science and Technology Committee of Fengxian District, Shanghai, China (No. FK20201501), the Natural Science Foundation of Shanghai, Shanghai, China (No. 22ZR1437600), the Health Commission of Huangpu District, Shanghai, China (No. HLQ202104), the Science and Technology Bureau of Kunshan, Suzhou, China (No. KS2252), and the Hainan Provincial Natural Science Foundation of China, Hainan, China (No. 823QN364).

CRediT authorship contribution statement

Yuxin Zhang: Writing – original draft, Methodology, Investigation, Formal analysis, Conceptualization. **Dahe Zhang:** Writing – original draft, Validation, Methodology, Investigation, Conceptualization. **Xin Jiao:** Validation, Software, Resources, Methodology, Investigation. **Xiaokun Yue:** Software, Methodology, Investigation, Data curation. **Bin Cai:** Resources, Methodology, Investigation, Data curation. **Shenji Lu:** Resources, Methodology, Investigation, Formal analysis. **Renjie Xu:** Writing – review & editing, Supervision, Funding acquisition, Formal analysis, Conceptualization.

Declaration of competing interest

The authors declare that they have no known competing financial interests or personal relationships that could have appeared to influence the work reported in this paper.

Acknowledgements

None.

List of abbreviations

SCI	spinal cord injury
OA	osteoarthritis
DEGs	differentially expressed genes
PPI	protein-protein interaction
WGCNA	weighted gene co-expression network analysis
TNF	tumor necrosis factor
IL	interleukin
GEO	Gene Expression Omnibus
GO	gene ontology
KEGG	Kyoto Encyclopedia of Genes and Genomes
TOM	topological overlap matrix

References

[1] S.A. Quadri, M. Farooqui, A. Ikram, A. Zafar, M.A. Khan, S.S. Suriya, C.F. Claus, B. Fiani, M. Rahman, A. Ramachandran, et al., Recent update on basic mechanisms of spinal cord injury, Neurosurg. Rev. 43 (2) (2020) 425–441.
[2] W. Ding, S. Hu, P. Wang, H. Kang, R. Peng, Y. Dong, F. Li, Spinal cord injury: the global incidence, prevalence, and disability from the global burden of disease study 2019, Spine 47 (21) (2022) 1532–1540.
[3] B. Abramoff, Caldera FE: **osteoarthritis: pathology, Diagnosis, and treatment options**, Med. Clin. 104 (2) (2020) 293–311.
[4] E.R. Vina, C.K. Kwoh, Epidemiology of osteoarthritis: literature update, Curr. Opin. Rheumatol. 30 (2) (2018) 160–167.
[5] G. Rodriguez, M. Berri, P. Lin, N. Kamdar, E. Mahmoudi, M.D. Peterson, Musculoskeletal morbidity following spinal cord injury: a longitudinal cohort study of privately-insured beneficiaries, Bone 142 (2021) 1–27.
[6] L.S. Lundell, M. Savikj, E. Kostovski, P.O. Iversen, J.R. Zierath, A. Krook, A.V. Chibalin, U. Widegren, Protein translation, proteolysis and autophagy in human skeletal muscle atrophy after spinal cord injury, Acta Physiol. 223 (3) (2018) 1–10.
[7] S. Abdelrahman, A. Ireland, E.M. Winter, M. Purcell, S. Coupaud, Osteoporosis after spinal cord injury: aetiology, effects and therapeutic approaches, J. Musculoskelet. Neuronal Interact. 21 (1) (2021) 26–50.
[8] X. Wu, X. Xu, Q. Liu, J. Ding, J. Liu, Z. Huang, Z. Huang, X. Wu, R. Li, Z. Yang, et al., Unilateral cervical spinal cord injury induces bone loss and metabolic changes in non-human primates (Macaca fascicularis), Journal of orthopaedic translation 29 (2021) 113–122.
[9] J. Lo, L. Chan, S. Flynn, A systematic review of the incidence, prevalence, costs, and activity and work limitations of amputation, osteoarthritis, rheumatoid arthritis, back pain, multiple sclerosis, spinal cord injury, stroke, and traumatic brain injury in the United States: a 2019 update, Arch. Phys. Med. Rehabil. 102 (1) (2021) 115–131.
[10] X. Liu, Y. Zhang, Y. Wang, T. Qian, Inflammatory response to spinal cord injury and its treatment, World neurosurgery 155 (2021) 19–31.
[11] V. Molnar, V. Matišić, I. Kodvanj, R. Bjelica, Ž. Jeleč, D. Hudetz, E. Rod, F. Čukelj, T. Vrdoljak, D. Vidović, et al., Cytokines and chemokines involved in osteoarthritis pathogenesis, Int. J. Mol. Sci. 22 (17) (2021) 9208.
[12] M.H.J. van den Bosch, Osteoarthritis year in review 2020: biology, Osteoarthritis Cartilage 29 (2) (2021) 143–150.
[13] Y. Gao, C. Mei, P. Chen, X. Chen, The contribution of neuro-immune crosstalk to pain in the peripheral nervous system and the spinal cord, Int. Immunopharm. 107 (2022) 1–10.
[14] X. Freyermuth-Trujillo, J.J. Segura-Uribe, H. Salgado-Ceballos, C.E. Orozco-Barrios, A. Coyoy-Salgado, Inflammation: a target for treatment in spinal cord injury, Cells 11 (17) (2022).
[15] P.G. Conaghan, A.D. Cook, J.A. Hamilton, P.P. Tak, Therapeutic options for targeting inflammatory osteoarthritis pain, Nat. Rev. Rheumatol. 15 (6) (2019) 355–363.
[16] B. Li, L.C. Tsoi, W.R. Swindell, J.E. Gudjonsson, T. Tejasvi, A. Johnston, J. Ding, P.E. Stuart, X. Xing, J.J. Kochkodan, et al., Transcriptome analysis of psoriasis in a large case–control sample: RNA-seq provides insights into disease mechanisms, J. Invest. Dermatol. 134 (7) (2014) 1828–1838.
[17] K. Yin, Y. Zhang, S. Zhang, Y. Bao, J. Guo, G. Zhang, T. Li, Using weighted gene co-expression network analysis to identify key modules and hub genes in tongue squamous cell carcinoma, Medicine 98 (37) (2019) 1–9.
[18] Y. Zhu, X. Ding, Z. She, X. Bai, Z. Nie, F. Wang, F. Wang, X. Geng, Exploring shared pathogenesis of Alzheimer's disease and type 2 diabetes mellitus via Co-expression networks analysis, Curr. Alzheimer Res. 17 (6) (2020) 566–575.
[19] M. Yao, C. Zhang, C. Gao, Q. Wang, M. Dai, R. Yue, W. Sun, W. Liang, Z. Zheng, Exploration of the shared gene signatures and molecular mechanisms between systemic lupus erythematosus and pulmonary arterial hypertension: evidence from transcriptome data, Front. Immunol. 12 (2021) 1–13.
[20] J. Li, G. Wang, X. Xv, Z. Li, Y. Shen, C. Zhang, X. Zhang, Identification of immune-associated genes in diagnosing osteoarthritis with metabolic syndrome by integrated bioinformatics analysis and machine learning, Front. Immunol. 14 (2023) 1134412.
[21] Q. Zhang, B. Yu, Y. Zhang, Y. Tian, S. Yang, Y. Chen, H. Wu, Combination of single-cell and bulk RNA seq reveals the immune infiltration landscape and targeted therapeutic drugs in spinal cord injury, Front. Immunol. 14 (2023) 1068359.
[22] S.P. Niu, Y.J. Zhang, N. Han, X.F. Yin, D.Y. Zhang, Y.H. Kou, Identification of four differentially expressed genes associated with acute and chronic spinal cord injury based on bioinformatics data, Neural regeneration research 16 (5) (2021) 865–870.
[23] L. Ji, X. Li, C. Zu, J. Li, X. He, Identification of a circRNA-mediated comprehensive ceRNA network in spinal cord injury pathogenesis, Experimental biology and medicine (Maywood, NJ) 247 (11) (2022) 931–944.
[24] Y.M. Ren, X. Zhao, T. Yang, Y.H. Duan, Y.B. Sun, W.J. Zhao, M.Q. Tian, Exploring the key genes and pathways of osteoarthritis in knee cartilage in a rat model using gene expression profiling, Yonsei Med. J. 59 (6) (2018) 760–768.
[25] M.E. Ritchie, B. Phipson, D. Wu, Y. Hu, C.W. Law, W. Shi, G.K. Smyth, Limma powers differential expression analyses for RNA-sequencing and microarray studies, Nucleic Acids Res. 43 (7) (2015) e47.
[26] Q. Zhu, Q. Li, X. Niu, G. Zhang, X. Ling, J. Zhang, Y. Wang, Z. Deng, Extracellular vesicles secreted by human urine-derived stem cells promote ischemia repair in a mouse model of hind-limb ischemia, Cell. Physiol. Biochem. 47 (3) (2018) 1181–1192.
[27] The gene ontology resource: 20 years and still GOing strong, Nucleic Acids Res. 47 (D1) (2019) D330–d338.
[28] M. Kanehisa, M. Furumichi, M. Tanabe, Y. Sato, K. Morishima, KEGG: new perspectives on genomes, pathways, diseases and drugs, Nucleic Acids Res. 45 (D1) (2017) D353–d361.
[29] D. Szklarczyk, A.L. Gable, D. Lyon, A. Junge, S. Wyder, J. Huerta-Cepas, M. Simonovic, N.T. Doncheva, J.H. Morris, P. Bork, et al., STRING v11: protein-protein association networks with increased coverage, supporting functional discovery in genome-wide experimental datasets, Nucleic Acids Res. 47 (D1) (2019) D607–d613.
[30] W. Liang, F. Sun, Weighted gene co-expression network analysis to define pivotal modules and genes in diabetic heart failure, Biosci. Rep. 40 (7) (2020).
[31] N.T. Doncheva, J.H. Morris, J. Gorodkin, L.J. Jensen, Cytoscape StringApp: network analysis and visualization of proteomics data, J. Proteome Res. 18 (2) (2019) 623–632.
[32] Z.Y. Song, F. Chao, Z. Zhuo, Z. Ma, W. Li, G. Chen, Identification of hub genes in prostate cancer using robust rank aggregation and weighted gene co-expression network analysis, Aging 11 (13) (2019) 4736–4756.
[33] Z. Huang, J. Shi, Y. Gao, C. Cui, S. Zhang, J. Li, Y. Zhou, Q. Cui, HMDD v3.0: a database for experimentally supported human microRNA-disease associations, Nucleic Acids Res. 47 (D1) (2019) D1013–d1017.
[34] C. Sticht, C. De La Torre, A. Parveen, N. Gretz, miRWalk: an online resource for prediction of microRNA binding sites, PLoS One 13 (10) (2018) 1–12.
[35] I.S. Vlachos, K. Zagganas, M.D. Paraskevopoulou, G. Georgakilas, D. Karagkouni, T. Vergoulis, T. Dalamagas, A.G. Hatzigeorgiou, DIANA-miRPath v3.0: deciphering microRNA function with experimental support, Nucleic Acids Res. 43 (W1) (2015) W460–W466.
[36] H. Ji, Y. Zhang, C. Chen, H. Li, B. He, T. Yang, C. Sun, H. Hao, X. Zhang, Y. Wang, et al., D-dopachrome tautomerase activates COX2/PGE(2) pathway of astrocytes to mediate inflammation following spinal cord injury, J. Neuroinflammation 18 (1) (2021) 130.
[37] Y. Zhang, Y. Zhou, S. Chen, Y. Hu, Z. Zhu, Y. Wang, N. Du, T. Song, Y. Yang, A. Guo, et al., Macrophage migration inhibitory factor facilitates prostaglandin E(2) production of astrocytes to tune inflammatory milieu following spinal cord injury, J. Neuroinflammation 16 (1) (2019) 85.
[38] X. Sang, X. Zhao, L. Yan, X. Jin, X. Wang, J. Wang, Z. Yin, Y. Zhang, Z. Meng, Thermosensitive hydrogel loaded with primary chondrocyte-derived exosomes promotes cartilage repair by regulating macrophage polarization in osteoarthritis, Tissue engineering and regenerative medicine 19 (3) (2022) 629–642.
[39] X. Qiao, W. Zhang, W. Zhao, Role of CXCL10 in spinal cord injury, Int. J. Med. Sci. 19 (14) (2022) 2058–2070.
[40] X.Y. Qiao, Y. Wang, W. Zhang, Q. Li, C. Liu, J.J. Dao, C.M. Qiao, C. Cui, Y.Q. Shen, W.J. Zhao, Involvement of CXCL10 in neuronal damage under the condition of spinal cord injury and the potential therapeutic effect of Nrg1, J. Integr. Neurosci. 22 (4) (2023) 96.
[41] G. Benigni, P. Dimitrova, F. Antonangeli, E. Sanseviero, V. Milanova, A. Blom, P. van Lent, S. Morrone, A. Santoni, G. Bernardini, CXCR3/CXCL10 Axis regulates neutrophil-NK cell cross-talk determining the severity of experimental osteoarthritis, J. Immunol. 198 (5) (2017) 2115–2124.

[42] L. Alcaide-Ruggiero, R. Cugat, J.M. Domínguez, Proteoglycans in articular cartilage and their contribution to chondral injury and repair mechanisms, Int. J. Mol. Sci. 24 (13) (2023).
[43] Z. Feng, K.J. Lian, Identification of genes and pathways associated with osteoarthritis by bioinformatics analyses, Eur. Rev. Med. Pharmacol. Sci. 19 (5) (2015) 736–744.
[44] H. Cao, P. Yang, J. Liu, Y. Shao, H. Li, P. Lai, H. Wang, A. Liu, B. Guo, Y. Tang, et al., MYL3 protects chondrocytes from senescence by inhibiting clathrin-mediated endocytosis and activating of Notch signaling, Nat. Commun. 14 (1) (2023) 6190.
[45] Z. Li, A. Dai, M. Yang, S. Chen, Z. Deng, L. Li, p38MAPK signaling pathway in osteoarthritis: pathological and therapeutic aspects, J. Inflamm. Res. 15 (2022) 723–734.
[46] D.Z. Tian, D. Deng, J.L. Qiang, Q. Zhu, Q.C. Li, Z.G. Yi, Repair of spinal cord injury in rats by umbilical cord mesenchymal stem cells through P38MAPK signaling pathway, Eur. Rev. Med. Pharmacol. Sci. 23 (3 Suppl) (2019) 47–53.
[47] G. Liu, B. Deng, L. Huo, S. Jiang, X. Fan, Y. Mo, J. Ren, Y. Zhao, L. Xu, X. Mu, Temporal profiling and validation of oxidative stress-related genes in spinal cord injury, Brain Res. Bull. 205 (2023) 110832.
[48] X. Weng, S. Maxwell-Warburton, A. Hasib, L. Ma, L. Kang, The membrane receptor CD44: novel insights into metabolism, Trends Endocrinol. Metabol.: TEM (Trends Endocrinol. Metab.) 33 (5) (2022) 318–332.
[49] L.J. Kang, J. Yoon, J.G. Rho, H.S. Han, S. Lee, Y.S. Oh, H. Kim, E. Kim, S.J. Kim, Y.T. Lim, et al., Self-assembled hyaluronic acid nanoparticles for osteoarthritis treatment, Biomaterials 275 (2021) 1–12.
[50] J. Yuan, B.O.A. Botchway, Y. Zhang, X. Tan, X. Wang, X. Liu, Curcumin can improve spinal cord injury by inhibiting TGF-β-SOX9 signaling pathway, Cell. Mol. Neurobiol. 39 (5) (2019) 569–575.
[51] I. Kurakazu, Y. Akasaki, H. Tsushima, T. Sueishi, M. Toya, M. Kuwahara, T. Uchida, M.K. Lotz, Y. Nakashima, TGFβ1 signaling protects chondrocytes against oxidative stress via FOXO1-autophagy axis, Osteoarthritis Cartilage 29 (11) (2021) 1600–1613.
[52] F. Li, B. Cheng, J. Cheng, D. Wang, H. Li, X. He, CCR5 blockade promotes M2 macrophage activation and improves locomotor recovery after spinal cord injury in mice, Inflammation 38 (1) (2015) 126–133.
[53] K. Takebe, M.F. Rai, E.J. Schmidt, L.J. Sandell, The chemokine receptor CCR5 plays a role in post-traumatic cartilage loss in mice, but does not affect synovium and bone, Osteoarthritis Cartilage 23 (3) (2015) 454–461.
[54] K. Kwiatkowski, K. Pawlik, K. Ciapała, A. Piotrowska, W. Makuch, J. Mika, Bidirectional action of cenicriviroc, a CCR2/CCR5 antagonist, results in alleviation of pain-related behaviors and potentiation of opioid analgesia in rats with peripheral neuropathy, Front. Immunol. 11 (2020) 615327.
[55] Y. Wang, X. Li, X. Xu, J. Yu, X. Chen, X. Cao, J. Zou, B. Shen, X. Ding, Clec7a expression in inflammatory macrophages orchestrates progression of acute kidney injury, Front. Immunol. 13 (2022) 1–10.
[56] W. Zhang, Q. Qiu, B. Sun, W. Xu, A four-genes based diagnostic signature for osteoarthritis, Rheumatol. Int. 41 (10) (2021) 1815–1823.
[57] H. Werner, The IGF1 signaling pathway: from basic concepts to therapeutic opportunities, Int. J. Mol. Sci. 24 (19) (2023).
[58] K.J. Allahdadi, T.A. de Santana, G.C. Santos, C.M. Azevedo, R.A. Mota, C.K. Nonaka, D.N. Silva, C.X.R. Valim, C.P. Figueira, W.L.C. Dos Santos, et al., IGF-1 overexpression improves mesenchymal stem cell survival and promotes neurological recovery after spinal cord injury, Stem Cell Res. Ther. 10 (1) (2019) 146.
[59] J.A. Collins, C.J. Kim, A. Coleman, A. Little, M.M. Perez, E.J. Clarke, B. Diekman, M.J. Peffers, S. Chubinskaya, R.E. Tomlinson, et al., Cartilage-specific Sirt6 deficiency represses IGF-1 and enhances osteoarthritis severity in mice, Ann. Rheum. Dis. 82 (11) (2023) 1464–1473.
[60] Z. Rasheed, N. Rasheed, W.A. Abdulmonem, M.I. Khan, MicroRNA-125b-5p regulates IL-1β induced inflammatory genes via targeting TRAF6-mediated MAPKs and NF-κB signaling in human osteoarthritic chondrocytes, Sci. Rep. 9 (1) (2019) 1–13.
[61] L. Yao, Y. Guo, L. Wang, G. Li, X. Qian, J. Zhang, H. Liu, G. Liu, Knockdown of miR-130a-3p alleviates spinal cord injury induced neuropathic pain by activating IGF-1/IGF-1R pathway, J. Neuroimmunol. 351 (2021) 1–10.
[62] B. He, D. Jiang, HOTAIR-induced apoptosis is mediated by sponging miR-130a-3p to repress chondrocyte autophagy in knee osteoarthritis, Cell Biol. Int. 44 (2) (2020) 524–535.
[63] X. Luo, J. Wang, X. Wei, S. Wang, A. Wang, Knockdown of lncRNA MFI2-AS1 inhibits lipopolysaccharide-induced osteoarthritis progression by miR-130a-3p/TCF4, Life Sci. 240 (2020) 1–12.
[64] J. Zhu, Y. Luo, Y. Zhao, Y. Kong, H. Zheng, Y. Li, B. Gao, L. Ai, H. Huang, J. Huang, et al., circEHBP1 promotes lymphangiogenesis and lymphatic metastasis of bladder cancer via miR-130a-3p/TGFβR1/VEGF-D signaling, Mol. Ther. : the journal of the American Society of Gene Therapy 29 (5) (2021) 1838–1852.
[65] F. Tian, J. Yang, R. Xia, Exosomes secreted from circZFHX3-modified mesenchymal stem cells repaired spinal cord injury through mir-16-5p/IGF-1 in mice, Neurochem. Res. 47 (7) (2022) 2076–2089.
[66] Q.C. Zhao, Z.W. Xu, Q.M. Peng, J.H. Zhou, Z.Y. Li, Enhancement of miR-16-5p on spinal cord injury-induced neuron apoptosis and inflammatory response through inactivating ERK1/2 pathway, J. Neurosurg. Sci. 68 (1) (2024) 101–108.
[67] X. Guo, X. Geng, Y. Chu, J. Gao, L. Jiang, MiR-204-5p alleviates neuropathic pain by targeting BRD4 in a rat chronic constrictive injury model, J. Pain Res. 15 (2022) 2427–2435.
[68] Y. Wang, F. Ye, C. Huang, F. Xue, Y. Li, S. Gao, Z. Qiu, S. Li, Q. Chen, H. Zhou, et al., Bioinformatic analysis of potential biomarkers for spinal cord-injured patients with intractable neuropathic pain, Clin. J. Pain 34 (9) (2018) 825–830.
[69] A. Srivastava, A.B. Dixit, D. Paul, M. Tripathi, C. Sarkar, P.S. Chandra, J. Banerjee, Comparative analysis of cytokine/chemokine regulatory networks in patients with hippocampal sclerosis (HS) and focal cortical dysplasia (FCD), Sci. Rep. 7 (1) (2017) 1–11.
[70] X. He, L. Deng, miR-204-5p inhibits inflammation of synovial fibroblasts in osteoarthritis by suppressing FOXC1, J. Orthop. Sci. : official journal of the Japanese Orthopaedic Association 27 (4) (2022) 921–928.
[71] X. Yang, H. Chen, H. Zheng, K. Chen, P. Cai, L. Li, K. Li, Y. Du, X.C. He, LncRNA SNHG12 promotes osteoarthritis progression through targeted down-regulation of miR-16-5p, Clin. Lab. 68 (1) (2022) 1–12.
[72] D. Li, Y. Sun, Y. Wan, X. Wu, W. Yang, LncRNA NEAT1 promotes proliferation of chondrocytes via down-regulation of miR-16-5p in osteoarthritis, J. Gene Med. 22 (9) (2020) 1–10.